

BNL--37328

DE86 005266

**MASTER**

**CONTACT MICROSCOPY WITH SYNCHROTRON RADIATION**

Barbara J. Panessa-Warren  
Department of Allied Health Resources and Anatomical Sciences  
State University of New York, Stony Brook  
Stony Brook, NY 11794

and

Instrumentation Division  
Brookhaven National Laboratory  
Upton, NY 11973-5000

**Suggested Running Title:**

**Soft X-Ray Contact Microscopy with Synchrotron Radiation**

October 1985

This research was partially supported by the U. S. Department of Energy. Contract No. DE-AC02-76CH00016, and in part by the NIH (NEI) Grant EYO-3422, the Retinitis Pigmentosa Foundation and the National Society to Prevent Blindness. By acceptance of this article, the publisher and/or recipient acknowledges the U.S. Government's right to retain a nonexclusive, royalty-free license in and to any copyright covering this paper.

*JSW*

## ABSTRACT

Soft x-ray contact microscopy with synchrotron radiation offers the biologist and especially the microscopist, a way to morphologically study specimens that could not be imaged by conventional TEM, STEM or SEM methods (i.e. hydrated samples, samples easily damaged by an electron beam, electron dense samples, thick specimens, unstained low contrast specimens) at spatial resolutions approaching those of the TEM, with the additional possibility to obtain compositional (elemental) information about the sample as well. Although flash x-ray sources offer faster exposure times, synchrotron radiation provides a highly collimated, intense radiation that can be tuned to select specific discrete ranges of x-ray wavelengths or specific individual wavelengths which optimize imaging or microanalysis of a specific sample. This paper presents an overview of the applications of x-ray contact microscopy to biological research and some current research results using monochromatic synchrotron radiation to image biological samples.

## INDEX ENTRIES

Biological soft x-ray contact microscopy; X-ray resists; Absorption edge imaging; Synchrotron radiation.

## DISCLAIMER

This report was prepared as an account of work sponsored by an agency of the United States Government. Neither the United States Government nor any agency thereof, nor any of their employees, makes any warranty, express or implied, or assumes any legal liability or responsibility for the accuracy, completeness, or usefulness of any information, apparatus, product, or process disclosed, or represents that its use would not infringe privately owned rights. Reference herein to any specific commercial product, process, or service by trade name, trademark, manufacturer, or otherwise does not necessarily constitute or imply its endorsement, recommendation, or favoring by the United States Government or any agency thereof. The views and opinions of authors expressed herein do not necessarily state or reflect those of the United States Government or any agency thereof.

The development of an imaging technique that exploited the properties of soft x-ray photons (1 - 10 nm wavelength) for studying biological material has continued since Lamarque (1936) (1) developed an x-ray generator capable of 1.2 nm wavelength radiation for biological microradiography. In the 1950's Engström (2,3) and Lindström (4) used ultrasoft x-rays to image cells and analyze various cell structures, developing the technique of "x-ray absorption microanalysis" with the construction of more, and increasingly versatile, synchrotrons biological contact microscopy could now be done with a more intense, collimated, tunable x-ray source. In the 1970's a group of scientists (5,6) imaged biological specimens using synchrotron broad band radiation around the carbon absorption edge by placing the biological specimen on a uniform layer of photoresist (polymethyl-methacrylate or PMMA); exposing the sample to x-radiation; washing away the biological tissue after x-ray exposure; and selectively removing the x-ray-damaged photoresist with solvents (such as methyl isobutyl ketone) resulting in the formation of a contour map or replica of the original specimen (Fig. 1). Because incident x-rays pass into the photoresist and damage it in areas where the biological sample does not cover the PMMA substrate, or where the biological sample is thin or has a low density, the x-ray contact replica that is formed by the solvent dissolution of these damaged areas reveals morphological and microchemical information with excellent fidelity and spatial resolution (Fig. 1). The resolution of the high molecular weight PMMA (2041) that is routinely used is approximately 5 nm when the resist is used optimally with photons of the wavelength just below the carbon absorption edge at 4.36 nm with a dosage of approximately  $10^4$  J/g (7).

The resolution of PMMA resist deteriorates at longer wavelengths because of increased diffraction effects and also deteriorates at shorter wavelengths due to the increased diameter of the shower of damaging particles in the resist (7). Other photoresists may be preferred when the intensity of the incident x-rays is too low for PMMA. Pianetta et al. (8) have used a faster resist polybutyl sulfone (PBS) as an imaging medium with moderate spatial resolution (~300 nm) for biological x-ray microscopy with monochromatic synchrotron radiation. Unfortunately most of the faster resists do not offer the high spatial resolution of PMMA (9). There are other acrylate resists, as well as novolak- and styrene-based x-ray resists. The styrene-based resists produce a negative image of the specimen with submicron resolution but accurate high resolution imaging is severely limited by swelling during solvent development (9). At present, for the biologist one of the most limiting factors for producing quality soft x-ray contact replicas is the x-ray resist itself. The difficulties in properly exposing, developing and viewing the x-ray resist are the major factors that limit resolution, fidelity of the image and information content of the biological sample.

#### The Replica

Once the x-ray exposure has been made, the sample is removed and the x-ray resist chemically developed. The development procedure is critical for biological imaging because the depth of development and such problems as under-cutting and overdeveloping must be avoided. The depth of development can be monitored by slowly, sequentially dissolving away the

resist in diluted solvent while monitoring the index of refraction color via light microscopy. Once the replica is developed it is coated with a thin layer of metal and usually examined by scanning electron microscopy (SEM). Due to the small submicron height of the features replicated in the x-ray resist, the higher the tilt angle during viewing, the more readily apparent the replicated biological structures will be and the crisper the micrographs of the surface topography. Many of the micrographs in this paper were taken at 65° to 74° tilt.

Recently by making silicon nitride windows supported by a silicon wafer frame, Feder et al. (10) has developed a way to mount the photoresist and sample on SiN<sub>3</sub> so that the final metal-coated x-ray replica can be viewed by transmission electron microscopy (TEM). This offers not only higher resolution imaging of the replica, but in future will permit the digitization of the replica image using scanning transmission electron microscopy (STEM) and direct high resolution image analysis using the state-of-the-art computer assisted software now available on analytical electron microscopes.

Since the x-ray contact replica is actually an atomic number/density topographical map of the original specimen, by using a short exposure to reduce specimen damage, and tuning the synchrotron radiation with a monochromator to obtain a specific x-ray wavelength, images can be made which reveal microchemical as well as morphological information (7,11,12). By comparing and measuring the differences in x-ray contact replica images made using two different x-ray wavelength exposures on either side of an absorption edge, information can be obtained on the

spatial distribution of specific elements in the periodic chart. In 1977, Petroff and Farge (13) successfully used this capability to map the distribution of transition metals in geological samples 30  $\mu\text{m}$  thick. Absorption edge imaging will be discussed in more detail and examples shown later in this paper.

#### Advantages of X-Ray Contact Microscopy in Biology

In 1952, Wolter (14) reported that in the region of 2.3 - 4.4 nm wavelength x-rays there is an order of magnitude difference between the absorption coefficients for water and protein. This difference in absorption coefficients provides a natural contrast mechanism to image biological hydrated specimens without requiring the use of such artificial means as fixation, chemical staining, or dessication followed by metal-coating (necessary when biological materials are viewed by conventional light and electron microscopy). In the x-ray wavelength range between 1 - 10 nm, theoretically biological specimens as thick as several microns can be successfully imaged using x-ray microscopy (7). This is in marked contrast to conventional TEM that requires thicknesses of approximately 50 - 300 nm. X-ray contact microscopy therefore cannot only image unstained, hydrated biological specimens with high contrast, but it also permits the examination of intact cells, droplet suspensions of cellular constituents and unsectioned preparations. When using an incident dose of soft x-rays the visibility of biological protein across structures in an aqueous medium in 1  $\mu\text{m}$  sections at  $10^4 \text{J/g}$  is calculated at 10 nm resolution, whereas only 70 nm resolution is calculated for imaging the same specimen at the same dose using electrons (7).

Therefore soft x-ray imaging offers a natural high contrast mechanism, and better spatial resolution, than electrons at the same dose.

#### Ideal Imaging Properties for Biological Samples

Biological samples are inherently difficult to image by conventional high resolution microscopy methods. Some tissues and intracellular components are extremely sensitive to ionizing radiation and show changes in surface morphology and molecular structure as soon as they are exposed to an electron beam (15). In mammals, one of the macromolecular building blocks of cartilage is the proteoglycan. These delicate, mutable aggregates and monomers seem to function in the hydration and transport of the cartilage matrix. Although their fine structure has been studied by pretreatment of isolated aggregates with cytochrome C, uranyl acetate or phosphotungstic acid, vacuum desiccation and Pt-metal coating (16,17), it has been difficult to correlate micrographs of these chemically-altered and desiccated samples to the original hydrated proteoglycans. Attempts at imaging freeze-dried proteoglycans using a  $-126^{\circ}\text{C}$  cryostage at the dedicated STEM at Brookhaven National Laboratory demonstrated that valid images were only obtainable with the first pass of the electron beam (dose  $23 \text{ e}^{-}/\text{A}^2$ , 40 kV accelerating voltage). By the second pass of the STEM beam most of the delicate side-chains of the monomer had been lost (Fig. 2). By x-ray contact microscopy, samples of proteoglycan aggregates resuspended in distilled water or diluted in buffer can be readily imaged without having to treat the specimen with fixatives stains or metal coatings. Figure 3 shows x-ray contact replicas of proteoglycan aggregates imaged using carbon x-rays ( $4.4 \text{ nm}\lambda$ ) from a stationary target

x-ray source ( $10^4 \text{J/cm}^2$ , 16 hour exposure time). Although these x-ray contact replicas are quite crisp and clearly show the hyaluronic acid backbone and the clumped side chains, the exposure period was long enough to raise questions about the possibility of specimen transformation or damage during the exposure (18,19). To reduce the exposure time and try to maintain the proteoglycans in their naturally hydrated state, similar preparations of isolate proteoglycan aggregates and monomer were imaged using a wet cell and soft x-rays from a flash x-ray source between 2.3 to 4.4 nm $\lambda$  at a 60 nsec exposure (20,21). With such a brief exposure time, the chances are significantly improved for imaging a biological specimen before damage has occurred. Even though the specimens were suspended in a 0.1  $\mu\text{l}$  droplet of water or dilute buffer during imaging (in a 125  $\mu\text{m}$  deep well in the wet cell chamber) both proteoglycan monomers and aggregates could be clearly seen (Fig. 4) and appear similar to the schematic (biochemical) representation of their structure. Although neither the micrographs in Figs. 3 or 4 were obtained from x-ray exposures at synchrotron sources, it is now possible to make x-ray exposures at specific band widths or x-ray wavelengths for relatively short periods of time to reduce biological specimen damage and preserve the more delicate and beam sensitive organic structures.

Occasionally morphological or compositional studies of biological samples that are heavily pigmented or inherently electron dense can present significant problems for the microscopist. Because image formation by x-ray contact microscopy is dependent on the differential absorption and transmission of incident x-rays, the optical density of a

specimen is not a limiting factor (22). Normally it is difficult to image the fine structure of any organelles masked by melanin accumulation in the cell. Figure 5 shows stained and unstained plastic sections of glutaraldehyde fixed frog retina pigment epithelium cells. My laboratory has been very interested in learning more about the fine structure of the pigment granules following light and dark adaptation. These pigment granules are so naturally electron dense (even in unstained sections) that conventional TEM and STEM reveal no information about the internal fibrillar or melanin structure. By x-ray contact microscopy of a similar plastic section of frog retina pigment epithelium, using synchrotron radiation (3.0 to 4.4 nm wavelength), there appears to be a globular internal structure of the pigment granules (Fig. 5). The x-ray replica shows a periodicity of 5 to 7 nm globules arranged in rows within the elliptical boundary of the granule (6,23). Because much thicker specimens can be imaged by x-ray contact microscopy than by conventional TEM and STEM, specimens that could only be viewed by high voltage electron microscopy (HVEM) can now be imaged with soft x-rays; without the severe specimen-beam damage (mass loss, heat damage) associated with HVEM, and with the advantage of gaining information about the atomic number composition and distribution in the sample.

#### Absorption Edge Imaging of Biological Samples

Because of the intensity, small source size and divergence of the synchrotron beam, and the ability to "tune" or select the band-width or wavelength(s) of the emitted x-rays exposing the resist (by using a monochromator), it is possible to make x-ray contact images of a sample

that optimally reveal the localization of specific elements within the sample. When identical samples are exposed to monochromatic x-rays whose wavelengths are on either side of the absorption edge of a specific element within the sample, two similar but not identical x-ray contact replicas are produced. The x-rays just above the absorption edge of the element in question will be absorbed by the specimen and not expose the underlying x-ray resist. The replica formed by exposing the sample to x-rays below the specific absorption edge will show x-ray penetration in the same areas (Fig. 6).

By comparing the two replicas made on either side of the absorption edge, information can be obtained about the spatial distribution of the element in question (7,11). According to the calculations of Kirz and Sayre (7), for an element to be detectable with a 10 nm spatial resolution at a dose of  $10^4$  J/g it must absorb a few percent of the incident x-radiation. "For elements with a major absorption edge in the 1 - 10 nm range (K edges  $4 < Z < 11$ , L edges for  $15 > Z < 30$ , M edges for  $38 < Z < 60$ ) this corresponds to detectable masses in the  $10^{-17}$  to  $10^{-18}$  g range or a concentration of 1 - 10% by weight in a 1  $\mu$ m thick specimen. For edges in the 0.1 - 1 nm range the radiation is more penetrating with the result that more mass ( $10^{-16}$  to  $10^{-17}$  g) is needed for detection" (7). This sort of detection sensitivity rivals electron beam induced conventional x-ray microanalysis. Although the biological sample for absorption edge imaging should ideally be flat, it need not be desiccated or embedded in plastic prior to exposure. Therefore, elemental loss and translocation, as well as contamination can be minimized and samples can

be imaged in a hydrated or frozen state in a wet cell or on a cold stage using extremely brief exposure periods. •

To demonstrate the type of images that can be obtained at specific absorption edges both sectioned tissue and subcellular components resuspended in buffer were used. Figure 7 shows the x-ray contact replicas produced by exposing plastic embedded gold (90 nm thick) sections of frog retina pigment epithelium (RPE) supported on copper grids to monochromatic x-rays (30.9 Å, nitrogen K absorption edge, 4 min 15 sec exposure). The copper grid bars and tissue section can be identified in the developed x-ray resist without any difficulty (Fig. 7a). Even folds in the section are faithfully reproduced in the resist material. At higher magnification the boundary between the nucleus and cytoplasm can be seen (arrows) but it is not clear whether the raised structure is truly the double nuclear membrane of the RPE cell. The adjacent cytoplasm appears to be filled with subcellular inclusions similar to the ribosomal aggregates and the extensive endoplasmic reticulum seen in stained TEM images of thin sections of the same RPE tissue (Fig. 7b). In an area of the section corresponding to Bruch's membrane some long narrow structures and intracellular material have been replicated (Fig. 7c) which may represent segments of collagen and mucopolysaccharides as well as cellular debris from the adjacent RPE. In this case, even though the tissue was fixed in glutaraldehyde (without post-fixation in osmium), dehydrated, embedded in plastic (EPON 812), sectioned and placed on 1 µm thick PMMA without any section staining to enhance image contrast, ultrastructural detail within the tissue section

is clearly replicated in the resist material. Since most intracellular structures contain nitrogen, using incident x-rays at the nitrogen absorption edge produced x-ray replicas with extensive morphological information about intracellular components. Ideally a second exposure should have been made of an identical section (on x-ray resist) using carbon x-rays to produce a typical ultrastructural image of the cell for comparison.

Going above and below a specific absorption edge can produce markedly different soft x-ray replicas. When isolated Limulus myosin filaments were prepared (in the laboratory of Dr. M. Dewey by homogenization, differential centrifugation, dialysis overnight against a relax buffer containing EDTA (4°C), resuspended in a low KCl Tris buffer pH 7.4 to 7.5) and replicated by exposing a 1 µl droplet on a PMMA coated silicon wafer using x-rays at 35.4 Å (the CaL<sub>II</sub> absorption edge) wavelength and 30.9 Å wavelength, two completely different sets of images were produced. Limulus telson levator muscle prepared using this procedure provides predominately elongate myosin filaments, and a few paramyosin paracrystals and actin filaments, as seen in the negatively stained (uranyl acetate) TEM image, Fig. 8. When a similar preparation was imaged with a flash x-ray source providing an exposure range of x-ray wavelengths from 2.3 to 4.4 nm the x-ray replica similarly revealed large paramyosin paracrystals (P) and myosin filaments (m) (Fig. 9a). However, when the same type of preparation was imaged using a monochromatic exposure at 30.9 Å wavelength, large clusters of globular material seem to be superimposed on filamentous structures (Fig. 9b). At 35.4 Å

wavelength exposures the same sample produced x-ray replicas that showed no filamentous structures or globular attached material. Some regions appeared to have absorbed the incident  $\text{CaL}_{11}$  edge x-rays (Fig. 10) and may be representative of regions where some residual calcium had still remained in the buffer or in association with the filaments and caused maximum absorption of the incident x-rays. The unusual, distinct replicas produced following  $30.9 \text{ \AA}$   $\lambda$  exposures may represent the myosin filaments decorated with Tris buffer (since the Tris is a high nitrogen buffer). Although this clearly demonstrates the potential of using monochromatic x-radiation for biological imaging and sample analysis, it also demonstrates the difficulties in specimen preparation, choice of incident radiation and interpretation of the data presented in the final replica.

#### Summary

Soft x-ray contact microscopy of biological samples using short exposures of x-rays with a specific wavelength, offers a completely new and powerful research tool to the biologist. Never before has it been possible to image living, hydrated and unstained biological specimens quickly enough to minimize sample deterioration and obtain high contrast images with high spatial resolution and compositional (elemental) information. Although this new type of microscopy has tremendous possibilities and potential, it is still quite new and requires great care and consideration in specimen preparation, resist development and interpretation of the final replica. The x-ray instrumentation (x-ray sources, monochromators, etc.) needed to do analytical and high

resolution spatial imaging of biological samples is already available. As in the early days of electron microscopy, today the major work that needs to be done to exploit these versatile x-ray techniques is in their application: in the areas of biological specimen preparation and studies of sample damage during exposure; x-ray resist and image recording technology; and image interpretation/validity. The present day synchrotrons offer the biologist who is inexperienced in x-ray technique, a ready supply of photons, and expertise in the form of resource personnel. Many of the presently operating synchrotrons produce sufficiently intense radiation to provide the brief exposures required for biological studies. The fact that synchrotron radiation is tuneable, and specific bands of x-ray wavelengths, or monochromatic radiation can be used for exposures makes possible many types of studies that could not be done with conventional visible light, electron or proton beam imaging/analytic methods. The radiation from the synchrotron is delivered to each beam port via a tube called a beam line. This configuration makes it possible to design specimen exposure chambers to be positioned in-front-of the beam port that permit maximum user accessibility and flexibility. Because of the large work area at the site of the beam port, cold stages, multi-sample holders, wet chambers and even microscopes (24) can be designed to utilize the synchrotron radiation emanating from the beam port itself, or the monochromator. This provides the investigator with a maximum of possibilities for the design of experiments and permits many analytical and microscopy techniques to be done at the same beam port. All that now remains is for biologists to begin using and exploring the vast possibilities of this versatile research tool.

Acknowledgements

The author is deeply indebted to Janos Kirz and the other scientists at the U15 beamline at the National Synchrotron Light Source at Brookhaven National Laboratory; Ralph Feder at IBM Watson Research Center; John Warren at Brookhaven National Laboratory; and Maynard Dewey and Elizabeth A. McGarvey of the Department of Anatomical Sciences at the State University of New York, Stony Brook for their willingness to share their expertise and assistance.

References

1. P. Lamarque, *Compt. Rend. Paris* 202, 684 (1936).
2. A. Engström, *Biochim. Biophys. Acta* 4, 351 (1950).
3. A. Engström, in *X-ray Microscopy and Microradiography*, V. Cosslett, A. Engström, and H. Pattee, Jr., eds., Academic Press, New York (1975), 24-38.
4. A. Engström and B. Lindström, *Biochim. Biophys. Acta* 4, 351 (1950).
5. E. Spiller, R. Feder, J. Topalian, D. Eastman, W. Gudat, and D. Sayre, *Science* 191, 1172 (1976).
6. R. Feder, E. Spiller, J. Topalian, A. N. Broers, W. Gudat, B. J. Panessa, J. Zadunaislay and J. Sedat, *Science* 197, 259 (1977).
7. J. Kirz and D. Sayre, in *Synchrotron Radiation Research*, S. Doniach, and H. Winick, eds., Plenum Press, New York (1980), 277-322.
8. P. Pianetta, R. Burg, J. Kurz, H. Rarback, J. McGowan and M. Malachowski, *X-ray Microscopy with the 4° Beam Line*, SSRL Report 79/01 (1979).
9. J. G. Lane, in *X-ray Lithography and Applications of Soft X-rays to Technology*, *Proc. of Intl. Soc. for Optical Engineer.*, A. Wilson, ed. 448, 119 (1983).
10. R. Feder and J. L. Costa, *Science* 212, 1398 (1981).
11. J. Wm. McGowan, B. Borwein, J. A. Medeiros, T. Beveridge, J. D. Brown, E. Spiller, R. Feder, J. Topalian, and W. Gudat, *J. Cell Biol.* 80, 732 (1979).
12. J. Wm. McGowan and M. J. Malachowski, *Ann. of New York Acad. of Sciences* 342, 288 (1980).

References (continued)

13. Y. Petroff and Y. Farge, *Appl. Phys. Lett.* 31, 785 (1977).
14. H. Wolter, *Ann. Phys. (Leipzig)* 10, 94 (1952).
15. B. J. Panessa, R. McCorkle, P. Hoffman, J. Warren, and G. Coleman, *Ultramicroscopy* 6, 139 (1981).
16. D. Heinegard, D. S. Lohmander, and J. Thyberg, *Biochem. J.* 175, 913 (1978).
17. L. Rosenberg, W. Hellmann, and A. Klein Schmidt, *J. Biol. Chem.* 250, 1877 (1975).
18. B. J. Panessa, J. B. Warren, P. Hoffman, and R. Feder, *Ultramicroscopy* 5, 267 (1980).
19. B. J. Panessa, G. Coleman, R. A. McCorkle, and J. B. Warren, *Scanning* 4, 21 (1981).
20. R. A. McCorkle, *J. Phys. B: Atom. Molec. Phys.* 11 (14), L407 (1978).
21. R. A. McCorkle, J. Angilello, G. Coleman, R. Feder, and S. J. LaPlaca, *Science* 205, 401 (1979).
22. B. J. Panessa-Warren, in *X-ray Microscopy*, G. Schmahl and D. Rudolph, eds., Springer Verlag, Berlin (1984), 268-278.
23. B. J. Panessa-Warren and J. B. Warren, *Ann. of New York Acad. of Sciences* 302 (1980).
24. J. Kirz and H. Rarback, *Rev. Sci. Instrum.* 56(1), 1 (1985).

FIGURE CAPTIONS

Figure 1 The biological specimen is placed on a 1  $\mu\text{m}$  thick PMMA (x-ray resist) coated silicon (Si) wafer (a) and exposed to soft x-rays. The soft x-rays are differentially absorbed by the specimen (according to the density and atomic number of the tissue), or the incident x-rays are transmitted through the biological material and selectively damage the underlying x-ray resist. After x-ray exposure, the biological specimen is removed, and the seemingly unaffected photoresist (b) is chemically treated to remove any regions damaged by the x-rays passing through, and around, the biological sample. The final developed replica (c) is raised (highest) in areas where x-ray transmission into the resist was reduced or prevented by the thickness of the specimen or by the presence of heavier atoms (high atomic number) within the tissue. Areas left in low relief where there is little resist remaining on the silicon wafer correspond to regions where the original specimen was thinner or comprised of low Z atoms thereby permitting greater x-ray penetration into the x-ray resist.

Figure 2 STEM images of proteoglycan monomer quench frozen in liquid nitrogen onto carbon substrates and imaged at  $-126^{\circ}\text{C}$ . During the first pass of the electron beam (a) the freeze-dried proteoglycans appear to have some discernable structure. However, by the second pass of the electron beam (b) much of the structure of the proteoglycans is gone due to mass loss and other beam induced damage.

Figure 3 Proteoglycan aggregates treated with cytochrome C were spread onto PMMA coated silicon wafers and exposed to carbon x-rays with a stationary target x-ray source (16 hour exposure). Many clusters of proteoglycan aggregates can be seen in the soft x-ray replica a. At higher magnification the complexity of the aggregates is apparent (b). A schematic diagram of a proteoglycan aggregate reveals a hyaluronic acid backbone with numerous branches of a protein core with chondroitin and keratin sulfate side chains (c).

Figure 4 Using a flash x-ray source, proteoglycan monomer (a) and aggregates (b) could be imaged in their hydrated condition in less than 60 nanoseconds. This type of rapid exposure soft x-ray replica reveals high resolution orphological information that is theoretically free of dehydration, movement and specimen damage artifacts.

Figure 5 A conventional heavy metal stained transmission electron micrograph of the apical portion of a retina pigment epithelial cell of the frog shows numerous elliptical, dense pigment granules (melanin) dispersed in the apical cytoplasm (a). Even in epithelial preparations in which the osmium and heavy metal stains have been excluded, the plastic embedded thin sections of these melanin granules are still electron dense and reveal no ultrastructural details (b). By carbon K x-ray imaging, the x-ray replicas of the frog retinal melanin granule reveals chains of 5 nm spherules running lengthwise

within the body of the elliptical granule (c). Since the contrast mechanism for soft x-ray contact microscopy is completely different than that for electron microscopy, x-ray microscopy can offer high resolution morphological information about electron dense structures that cannot be studied by conventional microscopy methods.

Figure 6 Identical biological samples can be imaged using monochromatic x-rays below and above a specific absorption edge. Below the absorption edge, the x-rays are maximally transmitted through the sample giving a low-relief replica (a). Just above the absorption edge (b), the x-rays are maximally absorbed by the element of interest in the specimen, thus producing an x-ray contact replica with high relief in the areas where the element of interest is located in the specimen (b). By comparing the two replicas, it is possible to identify the distribution of a specific element within a biological sample with better detection sensitivity than conventional electron beam-induced x-ray microanalysis for the lighter atomic number elements.

Figure 7 Monochromatic synchrotron radiation at 30.9 Å wavelength was used to image some plastic embedded thin sections of retina pigment epithelium. At low magnifications the grid bars and folded (arrow) section can be easily identified in the replica (a). At higher magnifications, the x-ray replica reveals minute ultrastructural details of the nucleus (N), nuclear

membrane (arrows) and the arrangement of membranous and ribosomal constituents of the cytoplasm (c) of the retina pigment epithelial cells (b). The nitrogen x-ray contact replica also reveals the formation and scattered appearance of the collagen (arrows) at the base of the retina pigment epithelium cells adjacent to Bruch's membrane (c).

Figure 8 Conventional negatively stained transmission electron microscopy of isolated Limulus muscle filaments reveals paramyosin, myosin (M) and very delicate actin filaments (A). This same muscle preparation was used to make the x-ray contact images shown in Figs. 9 and 10.

Figure 9 When Limulus isolated muscle filaments were imaged in their hydrated condition using a flash x-ray source (predominately 2.3 to 4.4 nmλ x-rays), the paramyosin and myosin (M) filaments were readily apparent (a). When a similar preparation with low calcium was imaged using monochromatic synchrotron radiation at 30.9 Å λ, the x-ray replica was remarkably different (b). Although some myosin filaments (arrows) can be seen in this nitrogen image (30.9 Å is the x-ray wavelength identified with the nitrogen absorption edge), the dilute Tris buffer in which the filaments were suspended seems to have produced an extensive decoration artifact around the filaments. Since Tris is a nitrogen buffer, it is understandable that it too was imaged when nitrogen x-rays were used for imaging. To clearly image the filaments a low salt acetate buffer could be effectively used.

Fig. 10 When an identical Limulus muscle filament preparation was used with monochromatic synchrotron radiation at  $35.4 \text{ \AA}$   $\lambda$  (CaL<sub>11</sub> edge), it was difficult to see any filaments in the replica. Although most of the free calcium in this muscle preparation had been removed by dialyzing with EDTA, some bound calcium is still present in the preparation. Most of the replica is covered with small aggregations of material (a) with larger highly raised amorphous regions (b) which may correspond to the areas of the sample with some remaining calcium. In any case, the replicas of the same isolated muscle preparation using 2.3 to 4.4 nm $\lambda$  x-rays is markedly different from both the nitrogen edge image at 3.09 nm and calcium L<sub>11</sub> edge image at 3.54 nm.

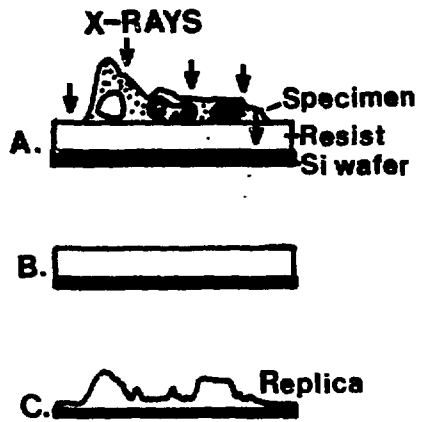


FIGURE 1

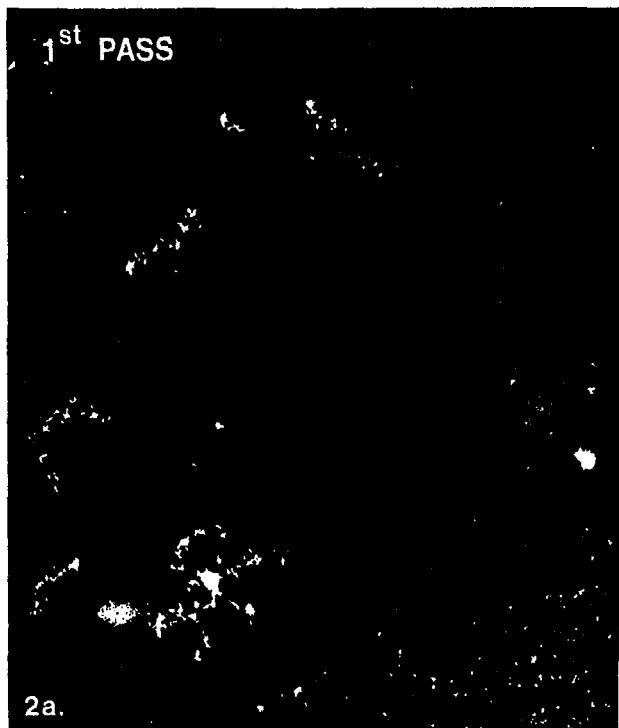


FIGURE 2

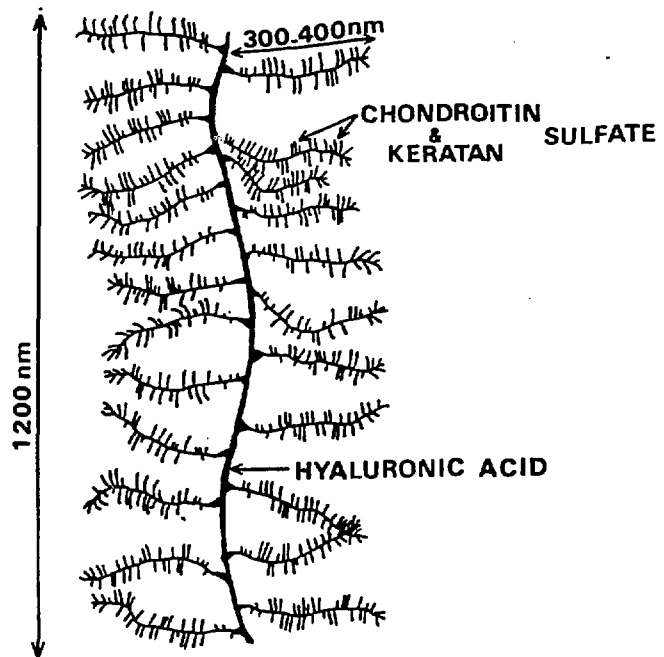
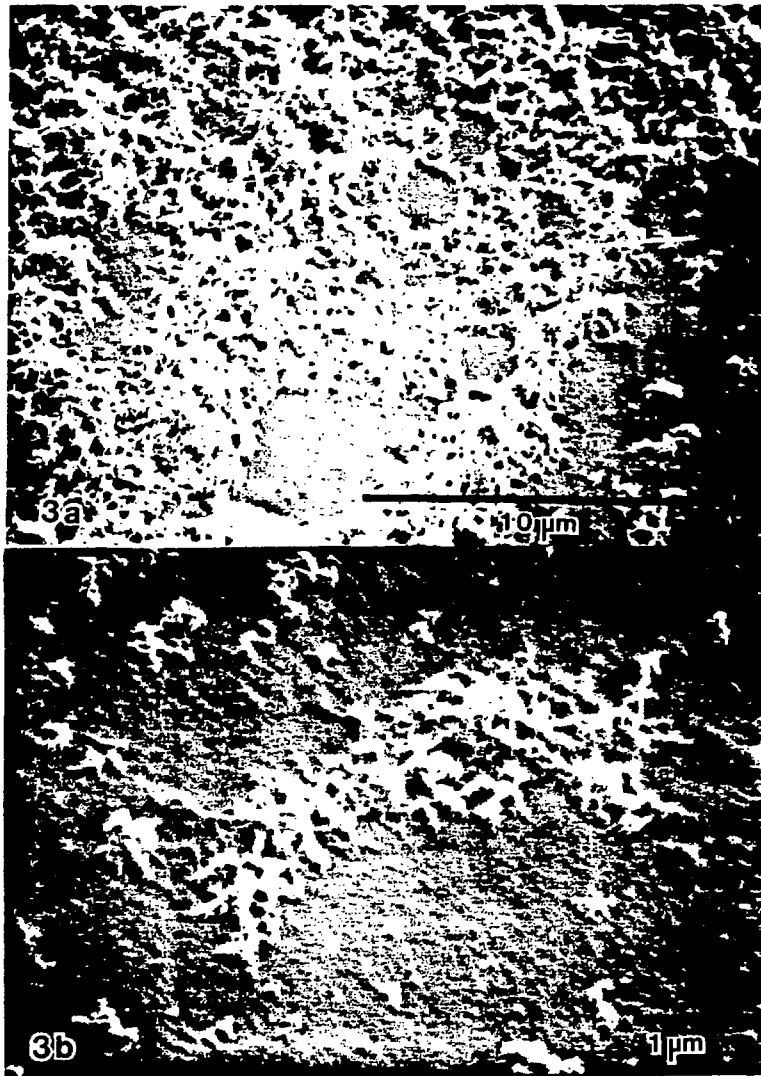


FIGURE 3

35

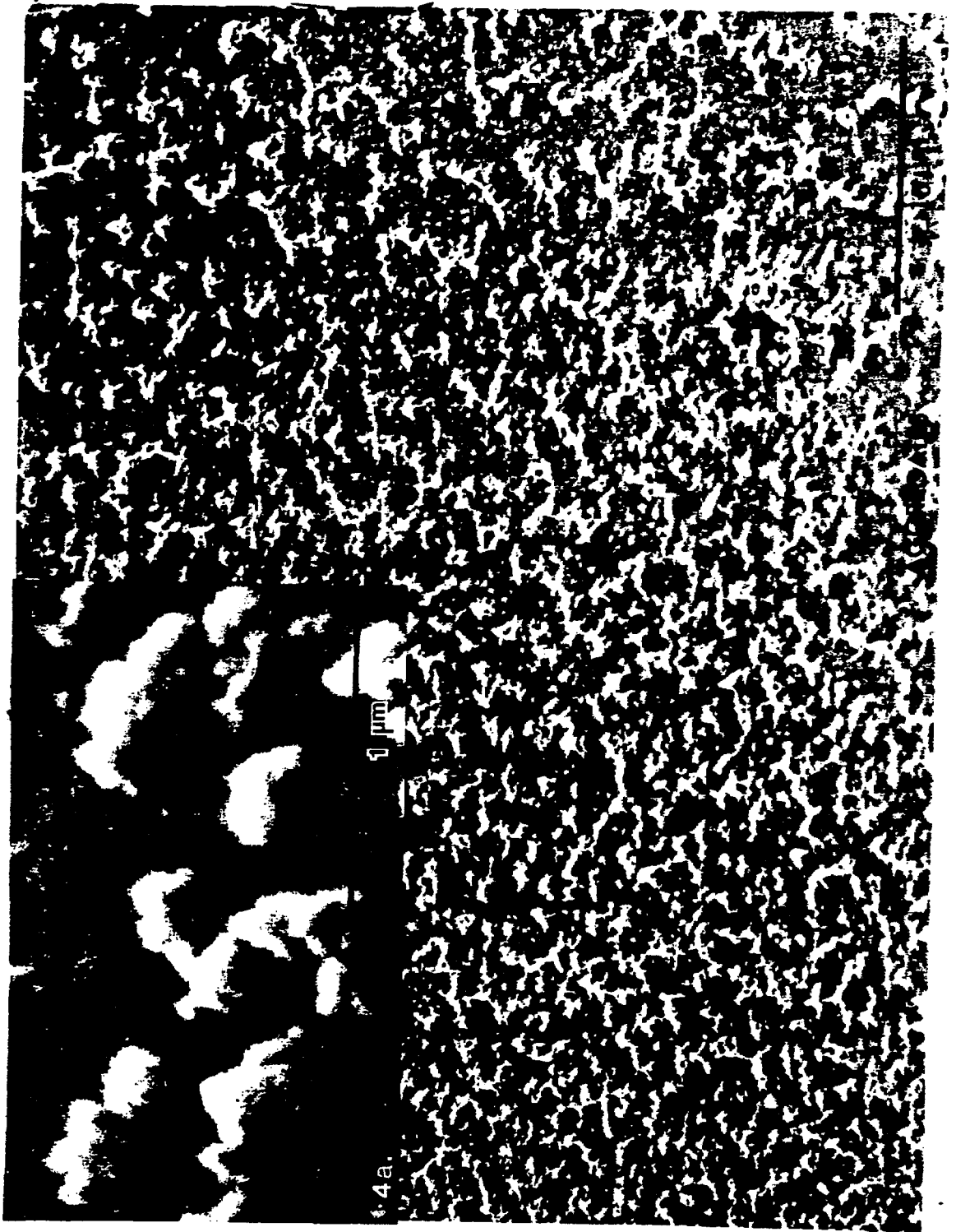


FIGURE 4



FIGURE 5

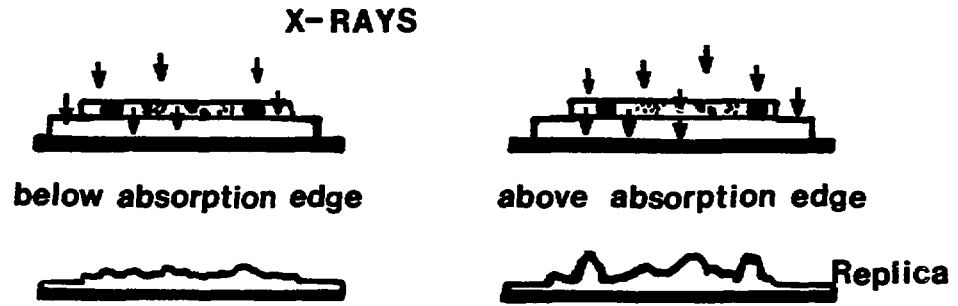


FIGURE 6

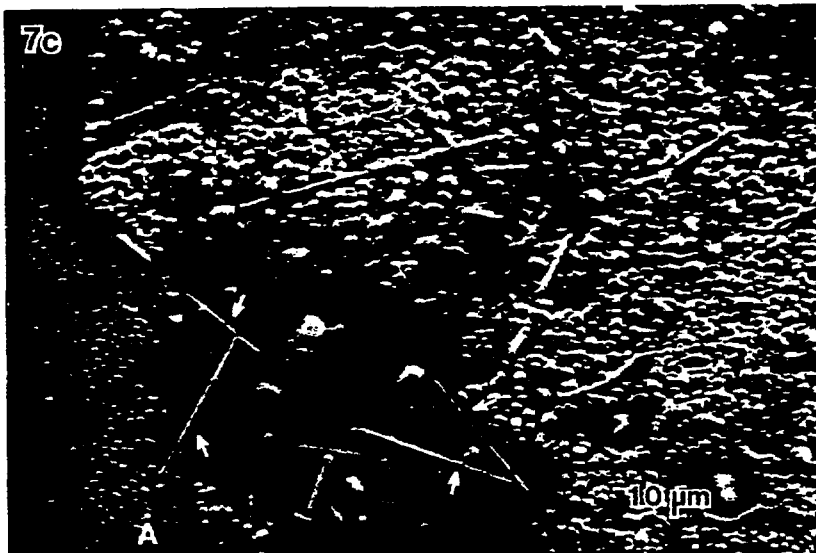
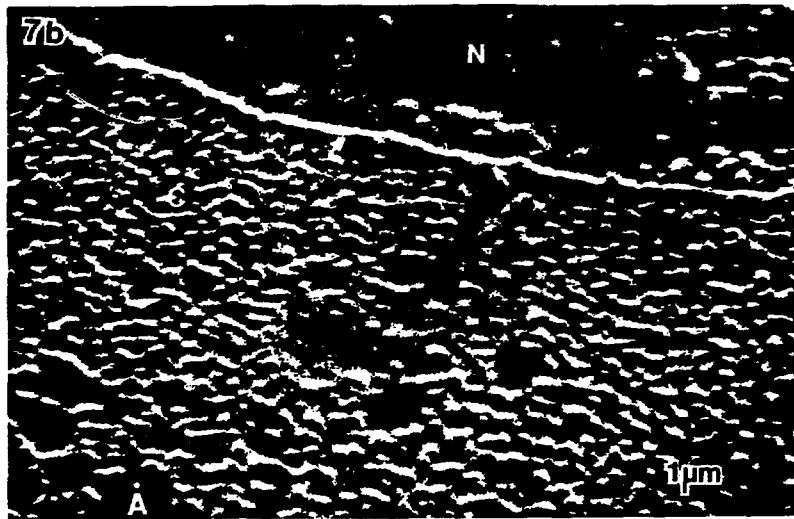
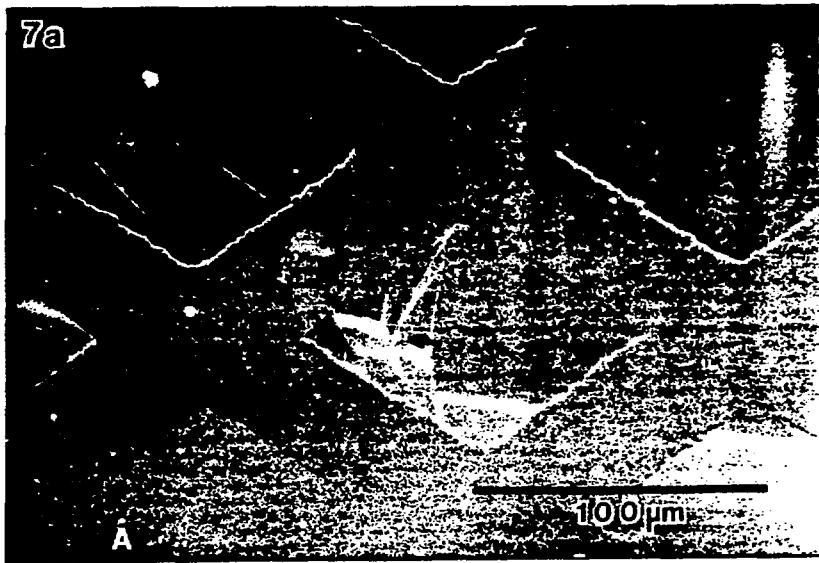


FIGURE 7



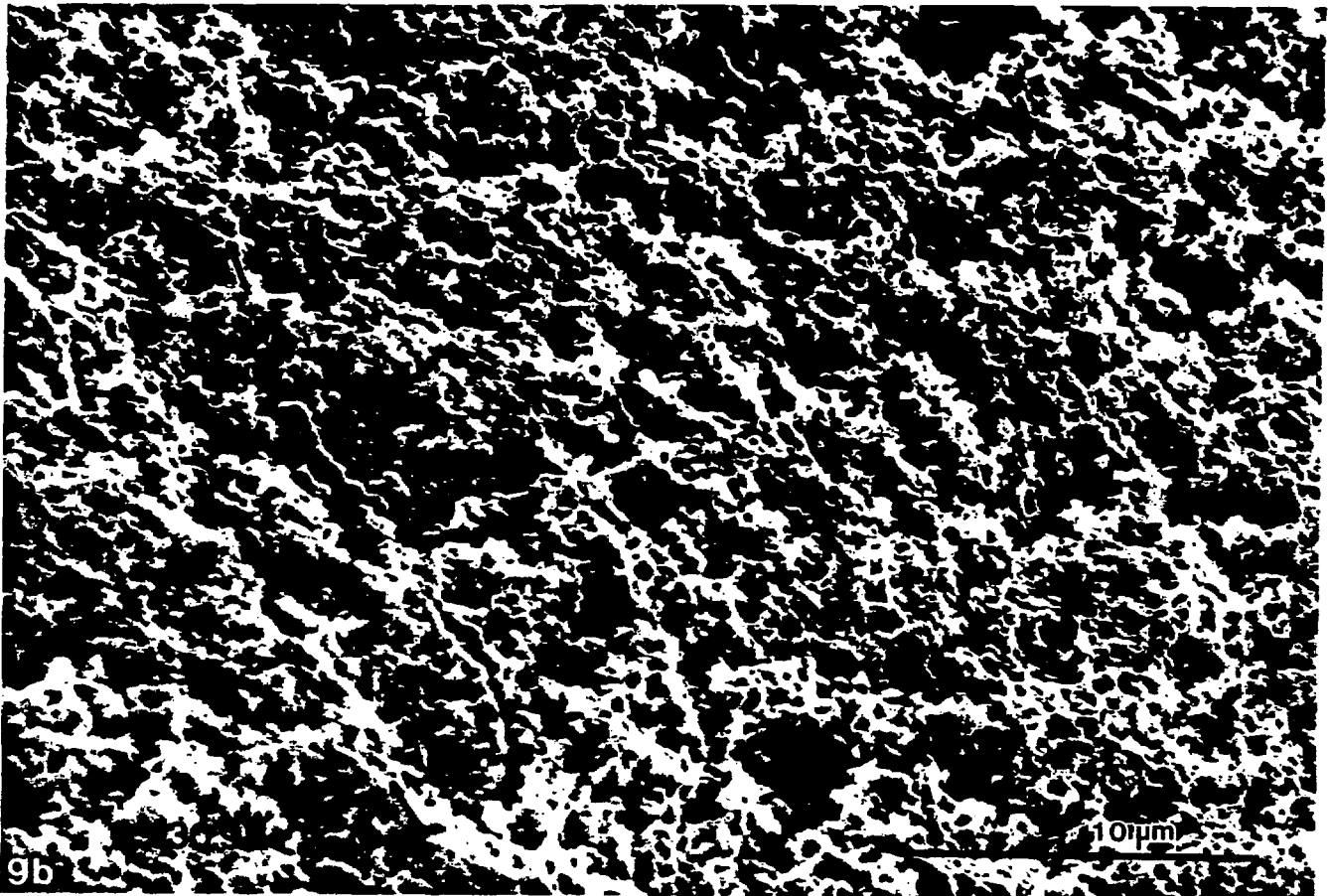


FIGURE 9

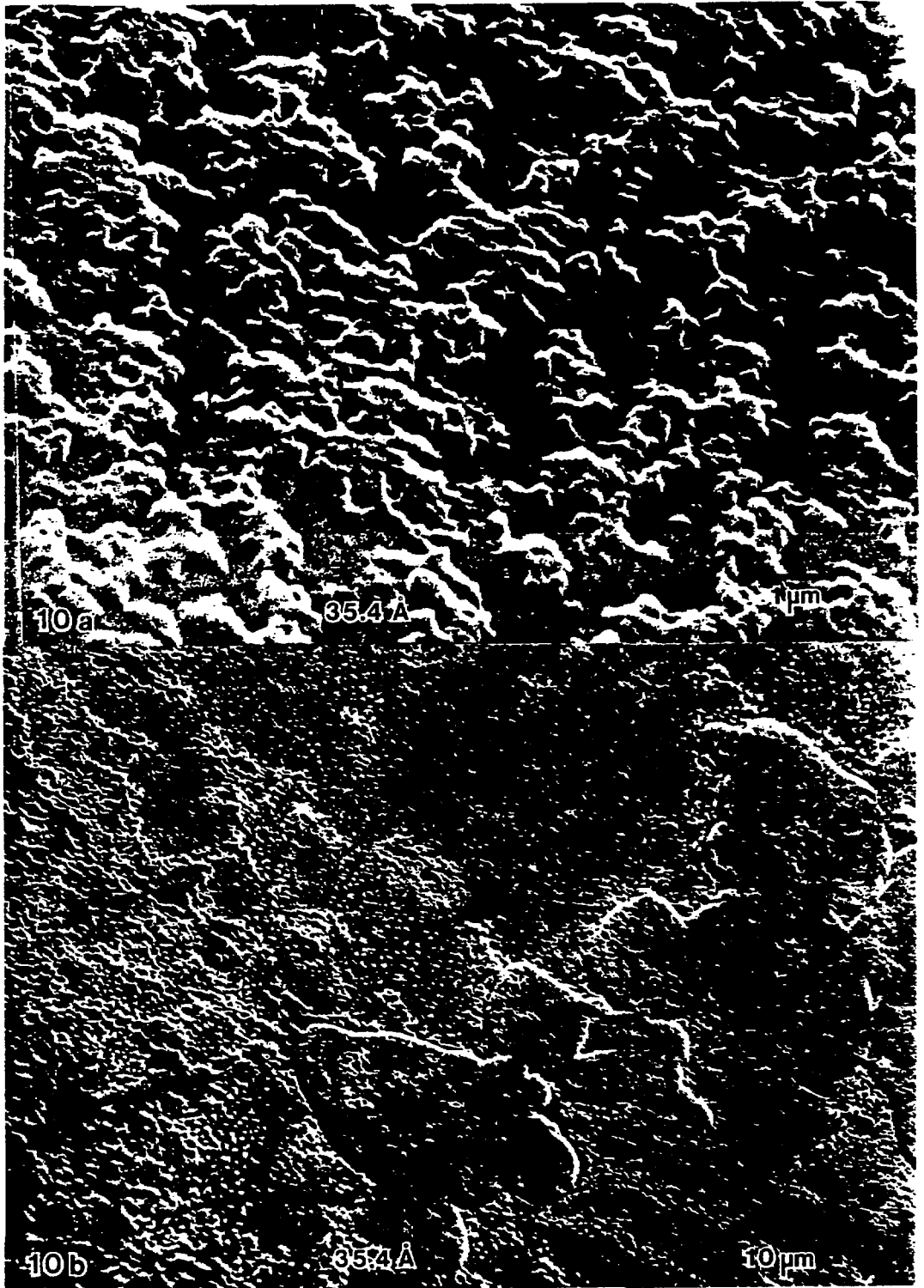


FIGURE 10